ACS APPLIED BIO MATERIALS

www.acsabm.org Article

Enhancing Electrochemical Biosensor Selectivity with Engineered D-Amino Acid Oxidase Enzymes for D-Serine and D-Alanine Quantification

Siba Moussa, Giulia Murtas, Loredano Pollegioni, and Janine Mauzeroll*

Cite This: *ACS Appl. Bio Mater.* 2021, 4, 5598−5604 Read Online

ACCESS | Metrics & More | Article Recommendations | Supporting Information

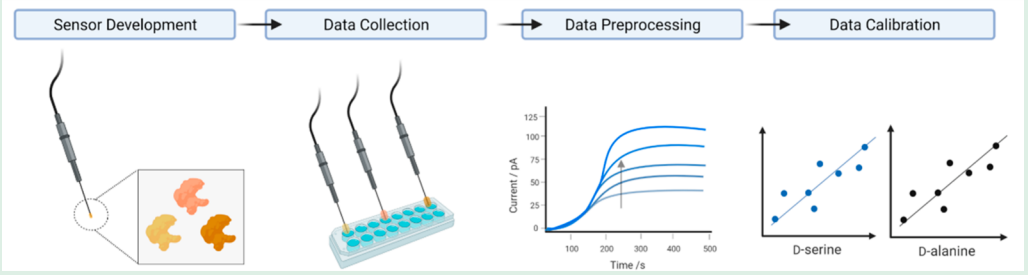

ABSTRACT: D-Amino acid oxidase (DAAO) enzymes bind a range of D-amino acids with variable affinity. As such, the design of selective DAAO-based enzymatic biosensors remains a challenge for real-world biosensor application. Herein, a methodology for developing biosensors with varying substrate selectivity is presented. First, we address DAAO-based biosensor selectivity toward D-serine by introducing point mutations into DAAO using rational design. Next, the wild-type yeast DAAO (*Rg*DAAO WT) and variants human DAAO W209R and yeast M213G are characterized for their selectivity and activity toward D-serine and D-alanine, the preferred DAAO substrates. The DAAO enzymes have been immobilized for final biosensor design, where they demonstrate selectivity comparable to free DAAO. The cross-linking procedure impacts on DAAO structure and function and the use of a regeneration strategy allows the biosensor response to be improved.

KEYWORDS: *biosensing, amino acids, cross-linking, proteins, peptides*

INTRODUCTION

D-Amino acids are increasingly reported for their roles in kidney function[1] and brain synaptic transmission regulation.[2] Altered D-amino acid levels, namely D-serine and D-alanine, are associated with disease prevalence such as kidney diseases,[3,4] schizophrenia,[5] and cancer,[6,7] making D-amino acids potential disease biomarkers.[8−10] To monitor and understand the role of D-serine and D-alanine in disease diagnosis,[5] management,[11] and treatment,[12,13] rapid online tracking of D-amino acid levels is essential.

The most employed method for D-amino acid detection is chromatography.[14−18] While useful for trace analyte detection, chromatography entails extensive sample preparation and long detection times and requires regular maintenance.[17,18] For clinical implementation, alternatives to chromatography should employ low-cost, rapid, and high-throughput measurements.[19] Biosensors are viable low-cost alternatives for analyte detection and quantification.[20] However, remaining improvement areas in biosensor design include analyte sensitivity and selectivity.

We previously demonstrated the application of D-amino acid oxidase (DAAO) biosensors for D-serine measurements in vivo.[21,22] These biosensors rely on DAAO surface immobilization onto a permselective polymer-modified platinum microelectrode (PPD-ME). DAAO is responsible for D-serine and D-alanine catalysis into equimolar amounts of hydrogen peroxide (H_2O_2),[23,24] which is oxidized at the ME polarized Pt surface (0.5 V). In practical application of D-serine biosensors, DAAO must preferentially detect D-serine among other substrates, especially in samples where D-alanine may also be present. Wild-type yeast *Rhodotorula gracilis* DAAO (*Rg*DAAO) is the classical enzyme used to develop DAAO-based biosensors. Using *Rg*DAAO WT-based biosensors, both D-alanine and D-serine are detected simultaneously.[21,25,26]

To increase DAAO-based biosensor selectivity and sensitivity, we use DAAO from different sources (variants) generated via protein engineering to produce biosensors with a range of analytical detection properties. DAAO variants share the same catalytic and kinetic mechanism (Scheme 1) while

Received: April 6, 2021
Accepted: June 8, 2021
Published: June 28, 2021

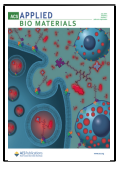

https://doi.org/10.1021/acsabm.1c00409
ACS Appl. Bio Mater. 2021, 4, 5598−5604

the rate constants associated with individual steps vary. Thus, kinetic constants for D-serine and D-alanine oxidation are impacted.

Scheme 1. Kinetic Mechanism of DAAO Enzymes[23,24a]

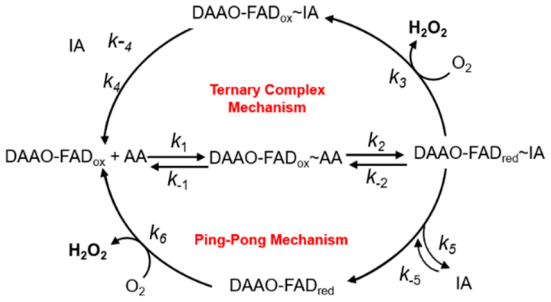

[a]The reaction can follow two kinetic mechanisms, i.e., ternary complex or ping-pong mechanism. AA, FAD_{ox}, FAD_{red}, and IA correspond to D-amino acid, oxidized FAD, reduced FAD, and imino acid, respectively. The rate constants for single steps depend on the DAAO enzyme type.

Using different DAAO enzymes (wild-type, M213G *Rg*DAAO[27,28] and the W209R variant of the human counterpart (*h*DAAO)[27,28]), we report the successful fabrication of three different biosensors with variable D-serine:D-alanine selectivity. Improving the detection properties of DAAO-based biosensors enable increased D-serine and D-alanine quantification accuracy. Moreover, we explore the mechanism in which immobilization impacts biosensor performance, noting that significant structural changes occur due to enzyme cross-linking. Finally, a unique biosensor strategy which increases biosensor lifetime is presented and the mechanism behind the regeneration principle is discussed.

EXPERIMENTAL SECTION

Chemicals. All reagents were purchased from Fischer Scientific or Sigma-Aldrich unless otherwise noted. All solutions were prepared using Millipore Milli-Q water (18.2 MΩ cm^{-1}).

Enzyme Preparation. Recombinant *Rg*DAAO WT (*Rg*DAAO, EC 1.4.3.3) was prepared as reported in literature.[29] Briefly, recombinant *Rg*DAAO WT was expressed in using the pT7-HisDAAO expression vector. Enzyme variants were selected by rational design. Recombinant *Rg*DAAO M213G variant was expressed using the pT7-HisDAAO M213G expression vector.[28] Recombinant *h*DAAO W209R was expressed using the pET11b-His *h*DAAO W209R expression vector.[30] Recombinant enzyme variants were produced in BL21(DE3)pLysS *E. coli* cells and purified to >90% purity. Enzymes were characterized using standard polarographic assays (0.253 mM O_2, 25 °C) with 28 mM D-alanine in 50 mM sodium pyrophosphate, pH 8.5 (containing 40 μM FAD for *h*DAAO W209R).[31] One enzyme unit is defined as the amount of enzyme that converts 1 μmol of D-amino acid per minute at 25 °C. Substrate specificity was investigated by a spectrophotometric assay based on detection of hydrogen peroxide production using a coupled assay with peroxidase and *o*-dianisidine (o-DNS, ε = 13 mM^{-1} cm^{-1}).[31] Pure enzymes were concentrated, stored in BSA and 1% glycerol, characterized using activity assays, and then used for the development of D-amino acid detecting biosensors (SI).

Biosensor Calibration, Storage, and Regeneration. In vitro calibrations in 0−50 μM D-serine or D-alanine in PBS (0.01 M, pH 7.4) were obtained using chronoamperometry (15 min, 0.5 V vs Ag/AgCl). Biosensors were stored at −20 °C dry. To test storage stability, biosensors were removed from storage, left for 10 min at room temperature in PBS, and calibrated using D-serine standard solutions (0−50 μM).

Biosensor regeneration capability was evaluated through the immersion of the biosensor in a solution of 1 mM D-serine. The biosensor was immersed for approximately 30 s under constant potential application (0.5 V) at the biosensor tip. The biosensor was then calibrated in standard D-serine solutions. The pre- and post-regeneration measurements were compared to quantify the impact of regeneration on the biosensor signal.

Characterizations of Free and Cross-Linked *Rg*DAAO. Free and crosslinked *Rg*DAAO were characterized using multiple characterization methods. Transmission electron microscopy (TEM) images were acquired using a Brightfield Philips CM200 TEM at 200 kV. Circular dichroism (CD spectra were recorded at 25 °C on a Jasco J-810 spectropolarimeter using a 1 cm path length cuvette. Infrared spectra were measured using a Fourier transform infrared (FTIR) spectrometer (Bruker) with attenuated total reflectance (ATR). A dynamic light spectrometer (DLS, Brookhaven instruments) was used to measure the particle size dispersion. Spectrophotometric measurements were performed using a thermostated UV/Vis spectrophotometer (V-560, Jasco) at 25 °C. Detailed experimental methodology on the characterization methods is presented in the Supporting Information.

Data Preprocessing, Analysis, and Statistics. All experimental data presented is the mean of triplicate measurements unless otherwise stated. Error bars represent the standard error of the mean (±SEM). Data was analyzed on either Excel 2013 or Python 3.7 and treated in Python 3.7. Error propagation calculations were performed on Python 3.7 All electrochemical signals were blank (PBS) signal corrected, resulting in i_{norm}. To generate the calibration curves, the steady state signals from noise-filtered data were extracted at each concentration and fit to a linear regression line. The limit of detection (LOD) corresponds to 3 times the standard deviation of the blank.[32] The limit of quantification (LOQ) corresponds to 10 times the standard deviation of the blank. The sensitivity was calculated from the slope of the regression fit. Selectivity toward D-serine was calculated as follows:

$$\text{Selectivity}_{D-ser} = \left[\frac{SA_{desiredproduct}}{SA_{undesiredproduct}}\right] \times 100 = \left[\frac{SA_{D-ser}}{SA_{D-ala}}\right] \times 100$$

where SA is the specific activity of the selected D-amino acid.

RESULTS AND DISCUSSION

DAAO Selection Strategy, Expression, and Characterization. Based on their reported kinetic properties (Table 1),[23,24,27,30] three DAAO enzymes were selected to develop biosensors with increased D-serine selectivity. Wild-type *h*DAAO (*h*DAAO WT) has a higher D-serine:D-alanine turnover ratio than the control wild-type *Rg*DAAO (*Rg*DAAO WT). Compared to the WT counterpart, *h*DAAO W209R has a higher turnover for both D-amino acids. *h*DAAO W209R also has a higher D-serine:D-alanine turnover ratio than both *Rg*DAAO WT and *h*DAAO WT. However, the M213G variant of *Rg*DAAO, previously identified as a DAAO variant with

Table 1. Apparent DAAO Kinetic Parameters at 25 °C, pH 8.5

enzyme	D-Ala k_{cat} (s^{-1})	D-Ser k_{cat} (s^{-1})	D-Ser:D-Ala turnover ratio	ref.
*h*DAAO WT	5.2	3.0	0.58	24
*Rg*DAAO WT	85	40.7	0.48	23
*h*DAAO W209R	11.8	7.2	0.61	30
*Rg*DAAO M213G	4.9	6.7	1.37	27

https://doi.org/10.1021/acsabm.1c00409
ACS Appl. Bio Mater. 2021, 4, 5598−5604

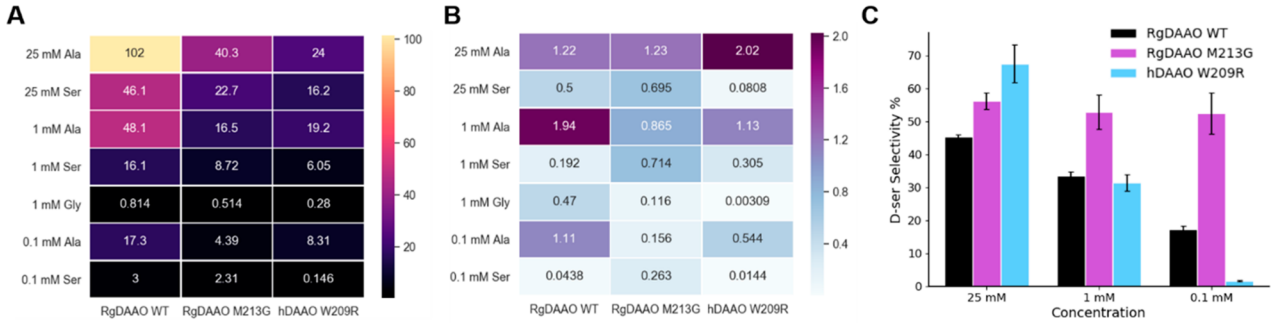

Figure 1. Characterization of *Rg*DAAO WT, *Rg*DAAO M213G, and *h*DAAO W209R using the spectrophotometric assay (pH 8.5). (A) Specific activity (U mg^{-1}) values for the enzymes at various substrate concentrations of D-serine, D-alanine, or glycine. (B) SEM values for the specific activities as reported in panel A. (C) Selectivity of enzymes toward D-serine over D-alanine. Error bars represent mean values ± SEM.

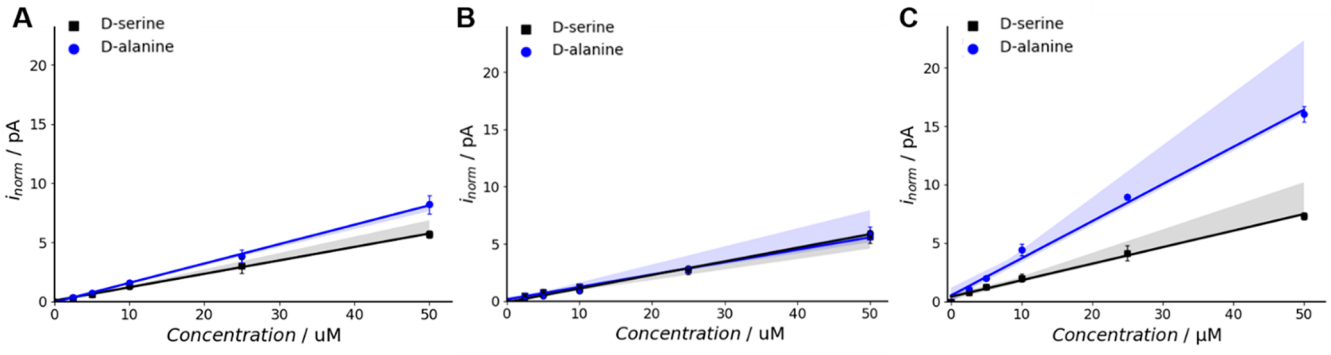

Figure 2. RgDAAO WT (A), RgDAAO M213G (B), and hDAAO W209R (C) biosensor calibration in standard solutions of 0−50 μM D-serine and D-alanine. Error bars represent ± S.E.M, (n = 3). The shaded area represent 95% confidence interval regions.

Table 2. Biosensor Calibration Parameters for the Various DAAO Enzymes Variants

	*Rg*DAAO WT		*Rg*DAAO M213G		*h*DAAO W209R	
	D-Ser	D-Ala	D-Ser	D-Ala	D-Ser	D-Ala
sensitivity (pA mM^{-1})	89.5 ± 1.52	154 ± 2.23	104 ± 5.61	117 ± 6.12	143 ± 3.42	291 ± 6.54
relative response at 50 μM (%)	63 ± 2.4	100 ± 0.30	80 ± 2.4	82 ± 4.2	80 ± 3.5	213 ± 5.3
			D-Ser selectivity (%)			
biosensor	63 ± 3.10		97.6 ± 1.75		37.6 ± 2.25	
free DAAO (100 μM)	17.3 ± 1.14		52.6 ± 6.29		1.75 ± 0.21	

improved catalytic activity on unnatural substrates, presents the highest D-serine:D-alanine turnover ratio.[27,28]

The selectivity and activity of DAAO enzymes were assessed via spectrophotometric activity assays on D-serine, D-alanine, and glycine (Figure 1). While all enzymes have negligible activity on glycine, enzyme activity toward D-serine and D-alanine varies with substrate concentration (as a result of different $K_{m,app}$ values). The substrate concentration-dependent enzyme activity affects the D-serine and D-alanine specificity of the enzyme. At saturating substrate conditions (25 mM), *h*DAAO W209R has the highest D-serine selectivity (i.e., the ratio of the experimental activity values on D-serine vs D-alanine) whereas at 0.1 mM, *h*DAAO W209R D-serine selectivity drops from 70% to 3% (Figure 1C).

While not possible to assay activity at substrate concentrations lower than 0.1 mM due to o-DNS assay sensitivity limitations, the results at 0.1 mM (a concentration in the higher range of in vivo biosensor application) indicate that *Rg*DAAO M213G is the most D-serine selective enzyme among the tested enzymes. The superior *Rg*DAAO M213G selectivity suggests the potential of its incorporation into biosensor design for enhanced D-serine detection as compared to previously published DAAO biosensors.[21,33,34]

DAAO Variants for Biosensor Development. Characterization of the free enzymes highlighted the potential of *Rg*DAAO M213G use for biosensor development. Yet, to fully compare *Rg*DAAO M213G performance against other DAAO enzymes in the final biosensor architecture, the free enzymes were used to build individual biosensors.

To develop biosensors with the different DAAO enzymes, the enzymes were immobilized on individual PPD-Pt MEs. Initial attempts of *h*DAAO W209R biosensor development were unsuccessful (Figure S1). As such, we established that enzyme concentrations >40 mg mL^{-1} are essential for biosensor design success (Figure S1A,D). Another factor important for biosensor success is the presence of FAD. *Rg*DAAO WT and *Rg*DAAO M213G show high FAD binding affinity ($K_d = 2 \times 10^{-8}$ M for *Rg*DAAO WT)[24,35,36] resulting in a tightly bound FAD which assures the presence of the active holoenzyme during enzyme immobilization. Conversely, *h*DAAO has a weak FAD binding affinity ($K_d = 2 \times 10^{-6}$),[37,38] making its exogenous presence a requirement in

https://doi.org/10.1021/acsabm.1c00409
ACS Appl. Bio Mater. 2021, 4, 5598−5604

biosensor design to avoid the production of the inactive apoprotein form. Although FAD coimmobilization with *h*DAAO W209R was ineffective at generating a linear calibration curve (Figure S1C), the presence of exogenous FAD (100 μM) in calibration solutions resulting in linear calibration curves (Figure S1B,D).

Biosensors were produced using enzyme concentrations of 56.8, 48, and 45 mg mL^{-1} for *Rg*DAAO WT, *Rg*DAAO M213G, and *h*DAAO W209R, respectively. Calibrations of all biosensors in standard D-serine and D-alanine solutions (Figure 2) indicate that each biosensor differs in selectivity and sensitivity toward D-serine and D-alanine (Table 2). Calibration curve regression parameters are listed in Table S1. Defining *Rg*DAAO WT's response to D-alanine as 100%, the relative response of all three biosensors toward D-serine and D-alanine is compared at 50 μM (Table 2).

As seen in the calibrations, the *h*DAAO W209R biosensor surpasses the performance of the other biosensors with respect to substrate response at 50 μM (D-ser, 80%; D-ala, 213%). Additionally, the *h*DAAO W209R biosensor supersedes the other biosensors in sensitivity (D-ala: 291 pA mM^{-1}) and D-alanine selectivity (62.4%, Table 2). Although the greatest in response when immobilized, the activity of free *h*DAAO W209R on D-serine and D-alanine is the lowest among other enzymes. The difference between free and immobilized *h*DAAO W209R responses suggests a strong impact of immobilization on enzyme behavior.

Additionally, both free and immobilized DAAO follow a similar trend for D-serine selectivity. Both DAAO forms demonstrate that *Rg*DAAO M213G has the greatest selectivity (55% free, 97.6% biosensor), followed by *Rg*DAAO WT (20% free, 63% biosensor), and finally *h*DAAO W209R (3% free, 37.6% biosensor). For free DAAO, the observed trend only applies at 0.1 mM substrate.

The results suggest that the free enzyme selectivity ratio at low substrate concentrations is a predictive parameter of biosensor selectivity. Thus, by characterizing free enzyme activity in the concentration range relevant to biosensor application, costs associated with enzymatic biosensor optimization are reduced. The biosensor performance may also be easily predicted.

Moreover, to evaluate the long-term enzyme stability following immobilization, biosensors were stored at −20 °C. After 2 weeks of storage, biosensors were calibrated and generated linear calibration curves with almost no change in the slope for *h*DAAO W209R. The sensitivity of *Rg*DAAO M213G and *Rg*DAAO WT, on the other hand, was impacted (Figure S2 and Table S2).

Immobilization Impacts DAAO Biosensor Performance. Despite reproducible biosensor fabrication methodology, each enzyme variant has its own intrinsic properties associated with structure−function relationships affecting biosensor performance. To understand the impact of the enzyme structure on the biosensor performance, we focus on the DAAO layer in the biosensor design. The DAAO layer in the biosensor represents a mixture of cross-linked DAAO and BSA aggregates. BSA is a highly hydrophilic protein used to stabilize enzymes.[39] BSA presence has no observed effect on enzyme activity (Table S3).

It is, however, the interenzyme differences that explain the reason behind *h*DAAO-biosensors surpassing the performance of other biosensors. Free *Rg*DAAO is a homodimer with head-to-tail interactions between the monomers[40] (Figure 3A),

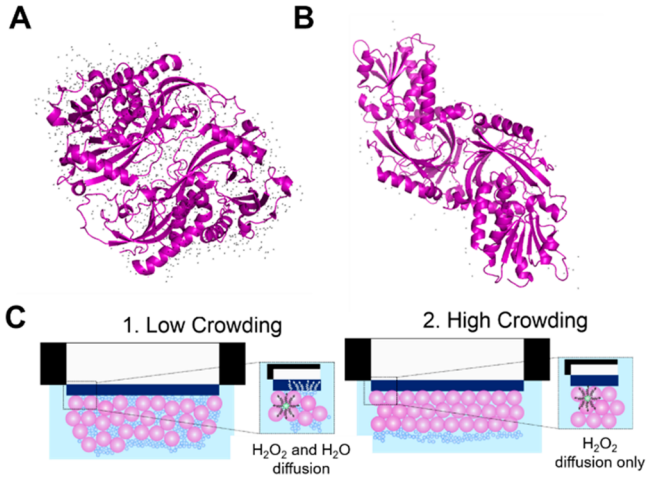

Figure 3. Structural representations of *Rg*DAAO WT and *h*DAAO WT and their interactions with surrounding nonbonded solvent molecules. The figures were prepared with PyMOL. (A) Crystal structure of *Rg*DAAO WT (dimer); the black dots correspond to the nonbonded water molecules (PDB code: 1C0P). *Rg*DAAO has a calculated 47.9% solvent accessible surface area. (B) Crystal structure of dimeric hDAAO WT; the black dots correspond to the nonbonded water molecules (PDB code: 2DU8). *h*DAAO is slightly more hydrophobic than *Rg*DAAO with a 43.0% solvent accessible surface area. (C) (1) Effect of *Rg*DAAO enzyme immobilization onto the microelectrode surface resulting in low crowding and allowing for the diffusion of both H_2O_2 and H_2O through the PPD layer. (2) Effect of *h*DAAO immobilization onto the microelectrode surface resulting in high crowding and low level of solvent molecules present near the electrode surface: this allows for the diffusion of only H_2O_2 produced by the enzyme close to the PPD layer.

whereas free *h*DAAO exists as a homodimer with head-to-head interactions between the monomers (Figure 3B).[41] *h*DAAO more hydrophobic than *Rg*DAAO (Figure 3A vs Figure 3B). *h*DAAO also has less polar contacts than *Rg*DAAO due to the net dipole moments of the molecules.

When immobilized onto the surface, and in comparison to *Rg*DAAO, the water molecules are not as tightly packed between the *h*DAAO enzyme molecules, creating a larger effective enzyme concentration (Figure 3C). The increased *h*DAAO effective concentration occurs due to a concept known as molecular crowding, a common biological phenomenon, occurring typically in cells. Molecular crowding may affect the enzyme stability, packing density, and oligomerization state.[42−44] As a result of molecular crowding and increased *h*DAAO stability, H_2O_2 production from the enzyme reaction rises and H_2O_2 diffusion toward the biosensor surface increases. As such, although the activity of free *h*DAAO is significantly lower on both D-serine and D-alanine than *Rg*DAAO (Table 1), *h*DAAO biosensors offer better limits of detection and sensitivities.[45−47]

In addition, structural changes which occur with glutaraldehyde cross-linking impact the immobilized enzyme behavior. Taking *Rg*DAAO WT for instance, circular dichroism (CD) spectra in the near UV range (Figure S3) suggest structural changes upon enzyme cross-linking. The CD spectral signals likely corresponding to phenylalanine (270−290 nm) and tryptophan (280−300 nm) residues vary between the free and the solution cross-linked DAAO. Moreover, ATR-FTIR spectra of glutaraldehyde, free *Rg*DAAO WT and cross-linked *Rg*DAAO WT demonstrate differences between the three

https://doi.org/10.1021/acsabm.1c00409
ACS Appl. Bio Mater. 2021, 4, 5598−5604

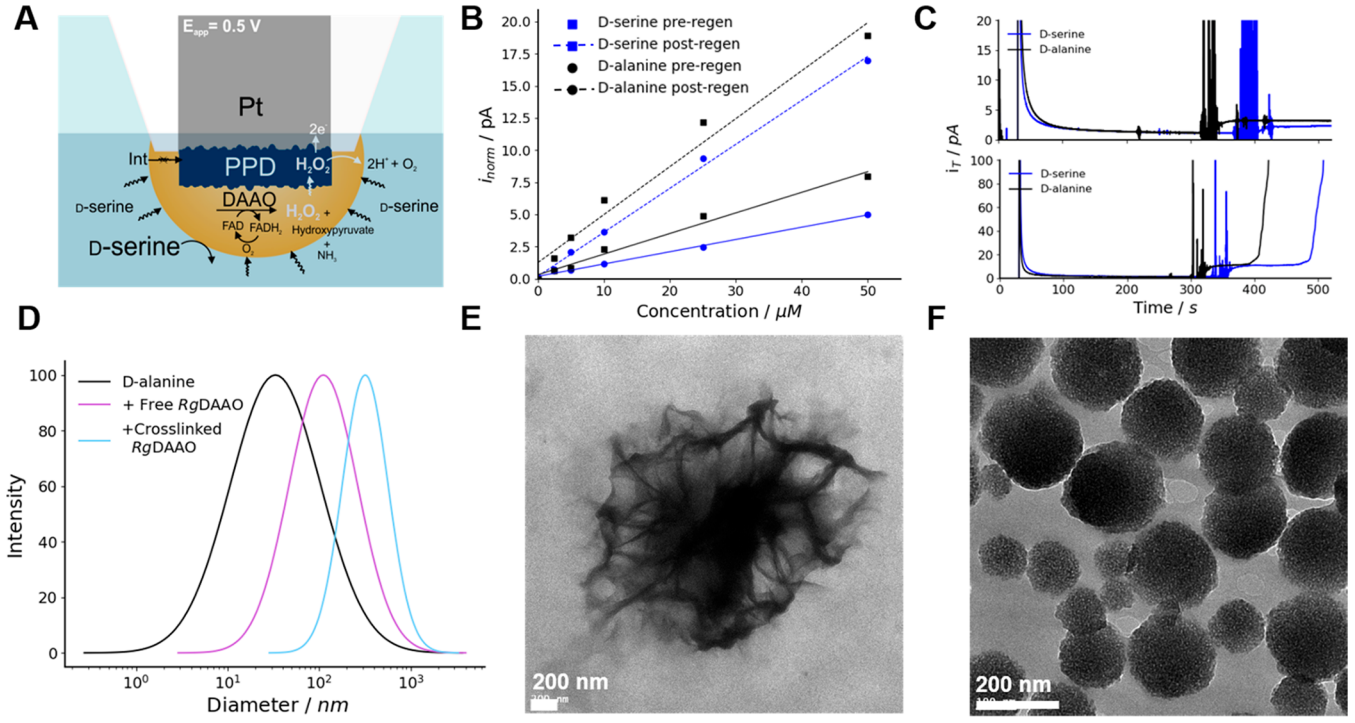

Figure 4. Biosensor regeneration strategy. (A) Scheme of biosensor placed in a solution of D-serine and the sequentially occurring reactions underlying D-serine detection. (B) Effect of biosensor regeneration on the calibration curve. (C) Electrochemical response of the biosensor in solutions of PBS added of 100 μM D-serine or D-alanine (top) and of 1 mM D-serine or D-alanine (bottom). (D) Laser light scattering size dispersion of 1 mM D-alanine, 0.5 μL of free *Rg*DAAO in 1 mM D-alanine, or 0.5 μL of cross-linked *Rg*DAAO in 1 mM D-alanine. (E) TEM image of immobilized *Rg*DAAO incubated in 100 μM D-alanine; scale bar: 200 nm. (F) TEM image of immobilized *Rg*DAAO incubated in 1 mM D-alanine; scale bar: 200 nm.

samples (Figure S4). The spectra for free and cross-linked *Rg*DAAO WT demonstrate changes in peaks for selected functional groups for the latter *Rg*DAAO form. The main distinctions can be made in four spectral regions: 3800−3300 cm^{-1} (O−H stretch), 3000−2800 cm^{-1} (C−H stretch), 1700−1500 cm^{-1} (N−H bend, C=C stretch), and 1450−1000 cm^{-1} (fingerprint region). Hence, it is evident that enzyme cross-linking alters certain enzyme functional groups, resulting in enzyme structural changes and impacting enzymatic biosensor performance.

Biosensors Can Be Regenerated with a Simple Strategy. For practical applications, biosensors must be easily regenerated after use. Regeneration is achievable through several mechanisms such as thermal heating, manual polishing, and chemical regeneration.[38] Chemical regeneration is the most widely used approach for biosensor regeneration taking advantage of enthalpic and entropic changes in solvent environment. Changes in the solvent environment include ionic strength, pH, and the presence of competitor ions, possible through use of regeneration buffers and acidic solutions.[38−40]

Using *Rg*DAAO WT as a prototype for DAAO biosensors, a novel biosensor regeneration strategy was developed. The biosensor was placed in a solution of 1 mM D-serine for a period of 30 s under simultaneous potential application to oxidize H_2O_2 (0.5 V) at the biosensor tip (Figure 4A). The biosensor was regenerated and the electrochemical signal was also amplified. Regeneration resulted in a 2.5-fold amplification of calibration curve steady-state currents (Figure 4B). The linear range is similar for pre and postregeneration calibrations (Table S4).

To explain the regeneration behavior, the biosensor electrochemical response was further explored. Immersed in 100 μM of substrate in PBS buffer, a steady current response is observed with the biosensor (Figure 4C, top). Immersed in 1 mM of substrate, the steady state current is also initially observed. However, after a period of 100−200 s a sudden burst in product formation occurs, characterized by over a 10-fold increase in the oxidation current (Figure 4C, bottom). The biosensor response at different substrate concentrations suggests microenvironment changes within the biosensor vicinity due to elevated H_2O_2 and H^+ ion levels around the enzyme layer (H^+ is the byproduct of H_2O_2 oxidation at the microelectrode surface), resulting in molecular crowding. The PPD layer rejects 70−80% of the H_2O_2 produced from diffusing toward the platinum sites.[21] As such, H_2O_2 and H^+ ion presence induce a pH change in the microenvironment of the enzyme layer, affecting both BSA and *Rg*DAAO tertiary conformation and spatial arrangement on the microelectrode surface.[48] In solution, the electrochemical behavior of free and cross-linked *Rg*DAAO WT is dissimilar to that of the biosensor, further supporting the presence of microenvironment changes only at the biosensor's enzyme-PPD interface (Figure S5).

Moreover, dynamic light scattering (DLS) measurements of free and cross-linked *Rg*DAAO in the presence of 1 mM D-alanine demonstrate aggregation and larger particle diameters for cross-linked *Rg*DAAO WT (Figures 4D and S6). Comparison of TEM images of cross-linked *Rg*DAAO incubated in D-alanine also demonstrate enzyme aggregation: the degree of aggregation, size, and morphology is tied to the D-alanine concentration (Figure 4E,F). Energy-dispersive X-ray

https://doi.org/10.1021/acsabm.1c00409
ACS Appl. Bio Mater. 2021, 4, 5598−5604

spectroscopy (EDS) analysis confirmed the presence of protein in the darker regions (Figure S7). The increased aggregation of cross-linked *Rg*DAAO suggests that enzyme aggregation plays a role in biosensor regeneration in addition to structural changes.[49,50]

CONCLUSION

Improving D-serine and D-alanine detection using enzymatic electrochemical biosensors is important for their practical application.[21] Significant improvements in biosensor sensitivity are owing to developments in the biorecognition elements. In this work, we altered the selectivity and specificity of the D-serine sensing element by using enzymes from different sources and variants, generated by point substitutions. The enzymes were successfully developed into DAAO-biosensors.

We also demonstrated that, while free enzyme activity does not necessarily define immobilized enzyme activity, it can serve as a predictive indicator for biosensor selectivity. Moreover, the cross-linking step in enzyme immobilization results in DAAO structural changes, enabling a simple biosensor regeneration strategy. Overall, this work enables the future development of DAAO biosensors with improved substrate selectivity and increased lifetimes. Future work consists of multiple biosensor application to quantify individual levels of D-serine and D-alanine in mixed substrate environments. These biosensors may be used to probe single or dual D-amino acid presence, enabling novel insights on D-amino acid function and roles in neurological disease onset and management.

ASSOCIATED CONTENT

Supporting Information

The Supporting Information is available free of charge at https://pubs.acs.org/doi/10.1021/acsabm.1c00409.

Detailed experimental methods and supplementary figures (PDF)

AUTHOR INFORMATION

Corresponding Author

Janine Mauzeroll − *Department of Chemistry, McGill University, Montreal, Quebec H3A 0B8, Canada;* orcid.org/0000-0003-4752-7507; Phone: 514-398-3898; Email: Janine.mauzeroll@mcgill.ca

Authors

Siba Moussa − *Department of Chemistry, McGill University, Montreal, Quebec H3A 0B8, Canada;* orcid.org/0000-0002-6873-2019

Giulia Murtas − *Dipartimento di Biotecnologie e Scienze della Vita, Università degli studi deII'Insubria, 21100 Varese, ltaly*

Loredano Pollegioni − *Dipartimento di Biotecnologie e Scienze della Vita, Università degli studi deII'Insubria, 21100 Varese, ltaly;* orcid.org/0000-0003-1733-7243

Complete contact information is available at: https://pubs.acs.org/10.1021/acsabm.1c00409

Author Contributions

All authors have given approval to the final version of the manuscript.

Notes

The authors declare no competing financial interest.

ACKNOWLEDGMENTS

This work was supposed by NSERC and MITACS. Part of this work was carried out by S.M. during a 3-month period at University of Insubria.

REFERENCES

(1) Kimura, T.; Hesaka, A.; Isaka, Y. Utility of D-Serine Monitoring in Kidney Disease. *Biochim. Biophys. Acta, Proteins Proteomics* **2020**, *1868* (9), 140449.

(2) Yamanaka, M.; Miyoshi, Y.; Ohide, H.; Hamase, K.; Konno, R. D-Amino Acids in the Brain and Mutant Rodents Lacking D-Amino-Acid Oxidase Activity. *Amino Acids* **2012**, *43* (5), 1811−1821.

(3) Hesaka, A.; Sakai, S.; Hamase, K.; Ikeda, T.; Matsui, R.; Mita, M.; Horio, M.; Isaka, Y.; Kimura, T. D -Serine Reflects Kidney Function and Diseases. *Sci. Rep.* **2019**, *9* (1), 1−8.

(4) Kimura, T.; Hamase, K.; Miyoshi, Y.; Yamamoto, R.; Yasuda, K.; Mita, M.; Rakugi, H.; Hayashi, T.; Isaka, Y. Chiral Amino Acid Metabolomics for Novel Biomarker Screening in the Prognosis of Chronic Kidney Disease. *Sci. Rep.* **2016**, *6* (1), 1−7.

(5) MacKay, M. A. B.; Kravtsenyuk, M.; Thomas, R.; Mitchell, N. D.; Dursun, S. M.; Baker, G. B. D-Serine: Potential Therapeutic Agent and/or Biomarker in Schizophrenia and Depression? *Front. Psychiatry* **2019**, *10* (FEB), 25.

(6) Bastings, J. J.A.J.; van Eijk, H. M.; Olde Damink, S. W.; Rensen, S. S. D-Amino Acids in Health and Disease: A Focus on Cancer. *Nutrients* **2019**, *11* (9), 2205−2223.

(7) Zhang, Z.; Liu, Y.; Liu, P.; Yang, L.; Jiang, X.; Luo, D.; Yang, D. Non-Invasive Detection of Gastric Cancer Relevant D-Amino Acids with Luminescent. *Nanoscale* **2017**, *9*, 19367.

(8) Lin, C. H.; Yang, H. T.; Chiu, C. C.; Lane, H. Y. Blood Levels of D-Amino Acid Oxidase vs. D-Amino Acids in Reflecting Cognitive Aging. *Sci. Rep.* **2017**, *7* (1), 1−10.

(9) Lin, C. H.; Yang, H. T.; Lane, H. Y. D-Glutamate, D-Serine, and D-Alanine Differ in Their Roles in Cognitive Decline in Patients with Alzheimer's Disease or Mild Cognitive Impairment. *Pharmacol., Biochem. Behav.* **2019**, *185*, 172760.

(10) Piubelli, L.; Pollegioni, L.; Rabattoni, V.; Mauri, M.; Princiotta Cariddi, L.; Versino, M.; Sacchi, S. Serum D-Serine Levels Are Altered in Early Phases of Alzheimer's Dis-Ease: Towards a Precocious Biomarker. *Transl. Psychiatry* **2021**, 01202.

(11) Kantrowitz, J. T.; Malhotra, A. K.; Cornblatt, B.; Silipo, G.; Balla, A.; Suckow, R. F.; D'Souza, C.; Saksa, J.; Woods, S. W.; Javitt, D. C. High Dose D-Serine in the Treatment of Schizophrenia. *Schizophr. Res.* **2010**, *121* (1−3), 125−130.

(12) Tsai, G. E.; Yang, P.; Chang, Y. C.; Chong, M. Y. D-Alanine Added to Antipsychotics for the Treatment of Schizophrenia. *Biol. Psychiatry* **2006**, *59* (3), 230−234.

(13) Kantrowitz, J. T.; Woods, S. W.; Petkova, E.; Cornblatt, B.; Corcoran, C. M.; Chen, H.; Silipo, G.; Javitt, D. C. D-Serine for the Treatment of Negative Symptoms in Individuals at Clinical High Risk of Schizophrenia: A Pilot, Double-Blind, Placebo-Controlled, Randomised Parallel Group Mechanistic Proof-of-Concept Trial. *Lancet Psychiatry* **2015**, *2* (5), 403−412.

(14) Kimura, R.; Tsujimura, H.; Tsuchiya, M.; Soga, S.; Ota, N.; Tanaka, A.; Kim, H. Development of a Cognitive Function Marker Based on D-Amino Acid Proportions Using New Chiral Tandem LC-MS/MS Systems. *Sci. Rep.* **2020**, *10* (1), 1−12.

(15) Furusho, A.; Koga, R.; Akita, T.; Mita, M.; Kimura, T.; Hamase, K. Three-Dimensional High-Performance Liquid Chromatographic Determination of Asn, Ser, Ala, and Pro Enantiomers in the Plasma of Patients with Chronic Kidney Disease. *Anal. Chem.* **2019**, *91* (18), 11569−11575.

(16) Nakano, Y.; Konya, Y.; Taniguchi, M.; Fukusaki, E. Development of a Liquid Chromatography-Tandem Mass Spectrometry Method for Quantitative Analysis of Trace D-Amino Acids. *J. Biosci. Bioeng.* **2017**, *123* (1), 134−138.

(17) Carenzi, G.; Sacchi, S.; Abbondi, M.; Pollegioni, L. Direct Chromatographic Methods for Enantioresolution of Amino Acids: Recent Developments. *Amino Acids*; Springer, 2020; pp 849−862.
(18) Xing, Y.; Li, X.; Guo, X.; Cui, Y. Simultaneous Determination of 18 D-Amino Acids in Rat Plasma by an Ultrahigh-Performance Liquid Chromatography-Tandem Mass Spectrometry Method: Application to Explore the Potential Relationship between Alzheimer's Disease and d-Amino Acid Level Alteration. *Anal. Bioanal. Chem.* **2016**, *408* (1), 141−150.
(19) Purohit, B.; Vernekar, P. R.; Shetti, N. P.; Chandra, P. Biosensor Nanoengineering: Design, Operation, and Implementation for Biomolecular Analysis. *Sensors Int.* **2020**, *1*, 100040.
(20) Shoja, Y.; Rafati, A. A.; Ghodsi, J. Enzymatic Biosensor Based on Entrapment of D-Amino Acid Oxidase on Gold Nanofilm/MWCNTs Nanocomposite Modified Glassy Carbon Electrode by Sol-Gel Network: Analytical Applications for D-Alanine in Human Serum. *Enzyme Microb. Technol.* **2017**, *100*, 20−27.
(21) Polcari, D.; Kwan, A.; Van Horn, M. R.; Danis, L.; Pollegioni, L.; Ruthazer, E. S.; Mauzeroll, J. Disk-Shaped Amperometric Enzymatic Biosensor for in Vivo Detection of D-Serine. *Anal. Chem.* **2014**, *86* (7), 3501−3507.
(22) Moussa, S.; Van Horn, M.; Shah, A.; Pollegioni, L.; Thibodeaux, C.; Ruthazer, E.; Mauzeroll, J. A Miniaturized Enzymatic Biosensor For Detection of Sensory-Evoked D-Serine Release in the Brain. *J. Electrochem. Soc.* **2021**, *168* (2), 025502.
(23) Pollegioni, L.; Langkau, B.; Tischer, W.; Ghisla, S.; Pilone, M. S. Kinetic Mechanism of D-Amino Acid Oxidases from Rhodotorula Gracilis and Trigonopsis Variabilis. *J. Biol. Chem.* **1993**, *268* (19), 13850−13857.
(24) Molla, G.; Sacchi, S.; Bernasconi, M.; Pilone, M. S.; Fukui, K.; Pollegioni, L. Characterization of Human D-Amino Acid Oxidase. *FEBS Lett.* **2006**, *580* (9), 2358−2364.
(25) Pernot, P.; Maucler, C.; Tholance, Y.; Vasylieva, N.; Debilly, G.; Pollegioni, L.; Cespuglio, R.; Marinesco, S. D-Serine Diffusion through the Blood-Brain Barrier: Effect on D-Serine Compartmentalization and Storage. *Neurochem. Int.* **2012**, *60* (8), 837−845.
(26) Van Horn, M. R.; Strasser, A.; Miraucourt, L. S.; Pollegioni, L.; Ruthazer, E. S. The Gliotransmitter D-Serine Promotes Synapse Maturation and Axonal Stabilization In Vivo. *J. Neurosci.* **2017**, *37* (26), 6277−6288.
(27) Caligiuri, A.; D'Arrigo, P.; Rosini, E.; Tessaro, D.; Molla, G.; Servi, S.; Pollegioni, L. Enzymatic Conversion of Unnatural Amino Acids by Yeast D-Amino Acid Oxidase. *Adv. Synth. Catal.* **2006**, *348* (15), 2183−2190.
(28) Sacchi, S.; Lorenzi, S.; Molla, G.; Pilone, M. S.; Rossetti, C.; Pollegioni, L. Engineering the Substrate Specificity of D-Amino-Acid Oxidase. *J. Biol. Chem.* **2002**, *277* (30), 27510−27516.
(29) Sonia, F.; Loredano, P.; Mirella, P. S. Engineering, Expression and Purification of a His-Tagged Chimeric D-Amino Acid Oxidase from Rhodotorula Gracilis. *Enzyme Microb. Technol.* **2001**, *29* (6−7), 407−412.
(30) Cappelletti, P.; Piubelli, L.; Murtas, G.; Caldinelli, L.; Valentino, M.; Molla, G.; Pollegioni, L.; Sacchi, S. Structure-Function Relationships in Human d-Amino Acid Oxidase Variants Corresponding to Known SNPs. *Biochim. Biophys. Acta, Proteins Proteomics* **2015**, *1854* (9), 1150−1159.
(31) Rosini, E.; Caldinelli, L.; Piubelli, L. Assays of D-Amino Acid Oxidase Activity. *Front. Mol. Biosci.* **2018**, *4*, 102.
(32) Long, G. L.; Winefordner, J. D. Limit of Detection: A Closer Look at the IUPAC Definition. *Anal. Chem.* **1983**, *55* (07), 712A−724A.
(33) Zain, Z. M.; O'Neill, R. D.; Lowry, J. P.; Pierce, K. W.; Tricklebank, M.; Dewa, A.; Ghani, S. A. Development of an Implantable D-Serine Biosensor for in Vivo Monitoring Using Mammalian d-Amino Acid Oxidase on a Poly (o-Phenylenediamine) and Nafion-Modified Platinum-Iridium Disk Electrode. *Biosens. Bioelectron.* **2010**, *25* (6), 1454−1459.
(34) Maucler, C.; Pernot, P.; Vasylieva, N.; Pollegioni, L.; Marinesco, S. In Vivo D-Serine Hetero-Exchange through Alanine-Serine-Cysteine (ASC) Transporters Detected by Microelectrode Biosensors. *ACS Chem. Neurosci.* **2013**, *4* (5), 772−781.
(35) Sacchi, S.; Lorenzi, S.; Molla, G.; Pilone, M. S.; Rossetti, C.; Pollegioni, L. Engineering the Substrate Specificity of D-Amino-Acid Oxidase* Downloaded From. *J. Biol. Chem.* **2002**, *277* (30), 27510−27516.
(36) Pollegioni, L.; Molla, G.; Sacchi, S.; Rosini, E.; Verga, R.; Pilone, M. S. Properties and Applications of Microbial D-Amino Acid Oxidases: Current State and Perspectives. *Appl. Microbiol. Biotechnol.* **2008**, *78*, 1−16.
(37) Caldinelli, L.; Iametti, S.; Barbiroli, A.; Bonomi, F.; Fessas, D.; Molla, G.; Pilone, M. S.; Pollegioni, L. Dissecting the Structural Determinants of the Stability of Cholesterol Oxidase Containing Covalently Bound Flavin. *J. Biol. Chem.* **2005**, *280* (24), 22572−22581.
(38) Pollegioni, L.; Sacchi, S.; Murtas, G. Human D-Amino Acid Oxidase: Structure, Function, and Regulation. *Front. Mol. Biosci.* **2018**, *5* (NOV), 107.
(39) Jeyachandran, Y. L.; Mielczarski, J. A.; Mielczarski, E.; Rai, B. Efficiency of Blocking of Non-Specific Interaction of Different Proteins by BSA Adsorbed on Hydrophobic and Hydrophilic Surfaces. *J. Colloid Interface Sci.* **2010**, *341* (1), 136−142.
(40) Umhau, S.; Pollegioni, L.; Molla, G.; Diederichs, K.; Welte, W.; Pilone, M. S.; Ghisla, S. The X-Ray Structure of D-Amino Acid Oxidase at Very High Resolution Identifies the Chemical Mechanism of Flavin-Dependent Substrate Dehydrogenation. *Proc. Natl. Acad. Sci. U. S. A.* **2000**, *97* (23), 12463−12468.
(41) Kawazoe, T.; Tsuge, H.; Pilone, M. S.; Fukui, K. Crystal Structure of Human D-Amino Acid Oxidase: Context-Dependent Variability of the Backbone Conformation of the VAAGL Hydrophobic Stretch Located at the Si -Face of the Flavin Ring. *Protein Sci.* **2006**, *15* (12), 2708−2717.
(42) Kuznetsova, I. M.; Turoverov, K. K.; Uversky, V. N. What Macromolecular Crowding Can Do to a Protein. *Int. J. Mol. Sci.* **2014**, *15*, 23090−23140.
(43) Ellis, R. J. Macromolecular Crowding: Obvious but Underappreciated. *Trends Biochem. Sci.* **2001**, *26*, 597−604.
(44) Lowe, M.; Kalacheva, M.; Boersma, A. J.; Kedrov, A. The More the Merrier: Effects of Macromolecular Crowding on the Structure and Dynamics of Biological Membranes. *FEBS J.* **2020**, *287*, 5039−5067.
(45) Goode, J. A.; Rushworth, J. V. H.; Millner, P. A. Biosensor Regeneration: A Review of Common Techniques and Outcomes. *Langmuir* **2015**, *31* (23), 6267−6276.
(46) Novotny, J.; Sharp, K. Electrostatic Fields in Antibodies and Antibody/Antigen Complexes. *Prog. Biophys. Mol. Biol.* **1992**, *58* (3), 203−224.
(47) Sahin, E.; Grillo, A. O.; Perkins, M. D.; Roberts, C. J. Comparative Effects of PH and Ionic Strength on Protein−Protein Interactions, Unfolding, and Aggregation for IgG1 Antibodies. *J. Pharm. Sci.* **2010**, *99* (12), 4830−4848.
(48) Gooding, J. J.; Pugliano, L.; Hibbert, D. B.; Erokhin, P. Amperometric Biosensor with Enzyme Amplification Fabricated Using Self-Assembled Monolayers of Alkanethiols: The Influence of the Spatial Distribution of the Enzymes. *Electrochem. Commun.* **2000**, *2* (4), 217−221.
(49) Xu, M. Q.; Li, F. L.; Yu, W. Q.; Li, R. F.; Zhang, Y. W. Combined Cross-Linked Enzyme Aggregates of Glycerol Dehydrogenase and NADH Oxidase for High Efficiency in Situ NAD+ Regeneration. *Int. J. Biol. Macromol.* **2020**, *144*, 1013−1021.
(50) Chen, Y.; Jiang, Q.; Sun, L.; Li, Q.; Zhou, L.; Chen, Q.; Li, S.; Yu, M.; Li, W. Magnetic Combined Cross-Linked Enzyme Aggregates of Ketoreductase and Alcohol Dehydrogenase: An Efficient and Stable Biocatalyst for Asymmetric Synthesis of (R)-3-Quinuclidinol with Regeneration of Coenzymes In Situ. *Catalysts* **2018**, *8* (8), 334.

https://doi.org/10.1021/acsabm.1c00409
ACS Appl. Bio Mater. 2021, 4, 5598−5604